
On the Effective Horizon of Inverse Reinforcement Learning

Yiqing Xu¹ Finale Doshi-Velez² David Hsu¹

¹National University of Singapore

²Harvard University

Abstract

Inverse reinforcement learning (IRL) algorithms often rely on (forward) reinforcement learning or planning over a given time horizon to compute an approximately optimal policy for a hypothesized reward function and then match this policy with expert demonstrations. The time horizon plays a critical role in determining both the accuracy of reward estimate and the computational efficiency of IRL algorithms. Interestingly, an *effective time horizon* shorter than the ground-truth value often produces better results faster. This work formally analyzes this phenomenon and provides an explanation: the time horizon controls the complexity of an induced policy class and mitigates overfitting with limited data. This analysis leads to a principled choice of the effective horizon for IRL. It also prompts us to reexamine the classic IRL formulation: it is more natural to learn jointly the reward and the effective horizon together rather than the reward alone with a given horizon. Our experimental results confirm the theoretical analysis.

1 Introduction

Inverse reinforcement learning (IRL) (Ng & Russell, 2000) aims to infer the underlying task objective from expert demonstrations. One common approach is to estimate a reward function that induces a policy matching closely the demonstrated expert trajectories. This model-based approach holds the promise of generalizing the learned reward function and the associated policy over unseen states (Osa et al., 2018).

Existing algorithms generally follow the classic IRL formulation and assume a known ground-truth discount factor, or equivalently, time horizon for the expert demonstrations (Ng & Russell, 2000; Abbeel & Ng, 2004; Ramachandran & Amir, 2007; Ziebart et al., 2008; Boularias et al., 2011; Levine et al., 2011; Wulfmeier et al., 2016; Pirotta & Restelli, 2016; Finn et al., 2016b,a; Ho & Ermon, 2016; Fu et al., 2018; Ni et al., 2020; Ke et al., 2020; Ramponi et al., 2020; Metelli et al., 2021; Hoshino et al., 2022). They then estimate a reward function, given the time horizon. Surprisingly, an *effective time horizon* shorter than the ground-truth value often produces better results faster. Why? Intuitively, the time horizon controls the complexity of an induced policy class. With limited data, a shorter time horizon is preferred, as the induced policy class is simpler and mitigates overfitting.

Further, the reward function and the time horizon capture two distinct aspects of the expert’s internal decision-making process. The reward function represents the expert’s task objective. The time horizon represents the expert’s strategic preference, *i.e.*, the relative importance of long-term and short-term reward. From this perspective, it is natural to learn jointly the reward and the time horizon together, rather than the reward alone with a given horizon, as the expert’s decision horizon is generally unknown in practice.

In this work, we present a formal analysis showing that with limited expert demonstrations, a reduced discount factor or time horizon improves the generalization performance of the learned reward function over unseen states. Based on this result, we propose to learn the reward function and the discount factor jointly. We describe a simple extension of the linear programming IRL algorithm (LP-IRL) (Ng & Russell, 2000) and the maximum entropy IRL algorithm (MaxEnt-IRL) (Ziebart et al., 2008) to do so through cross-validation. Our experimental evaluation of both LP-IRL and MaxEnt-IRL on four different tasks support our theoretical analysis.

We are not aware of prior work that formally analyzes the relationship between the time horizon and the performance of the learned reward function in IRL. Some IRL algorithms employ a smaller effective time horizon for computational efficiency, albeit at the cost of myopic sub-optimal policies (MacGlashan & Littman, 2015; Lee et al., 2022; Xu et al., 2022). The work of Jiang et al. (2015) shows that for planning in a Markov decision process, a shorter horizon improves the policy performance, when the dynamic model is inaccurate. It is, however, unclear whether a similar phenomenon about the horizon occurs in IRL, where the reward function is unknown and estimated from expert data.

2 Related works

Effective Horizon of Imitation Learning Imitation learning learns desired behaviors by imitating expert demonstrations and comprises two classes of methods: model-free behavior cloning (BC) and model-based inverse reinforcement learning (IRL) (Osa et al., 2018). The primary distinction between BC and IRL lies in the horizons used to align the learned behaviors with expert data. BC matches step-wise expert actions, resulting in poor generalization to unseen states. In contrast, IRL addresses this issue by either matching multi-step trajectory distributions (Ziebart et al., 2008; Boularias et al., 2011; Levine et al., 2011; Wulfmeier et al., 2016; Finn et al., 2016b,a; Pirota & Restelli, 2016; Ramponi et al., 2020), or their marginalized approximations (Ho & Ermon, 2016; Fu et al., 2018; Ni et al., 2020; Ke et al., 2020; Ghasemipour et al., 2019; Hoshino et al., 2022). The former employs a double-loop structure to interleave the policy optimization and reward function update, while the latter learns a discriminator to distinguish expert-like behaviors. Both approaches utilize the ground-truth horizon/discount factor for optimization, ensuring global temporal consistency between the learned policy and expert. Notably, few IRL methods adopt receding horizons to reduce computational cost (MacGlashan & Littman, 2015; Lee et al., 2022; Xu et al., 2022), claiming shorter optimization horizons yields sub-optimal policies. However, a theoretical analysis on the impact of the horizon choice in IRL is lacking, making it an important yet overlooked consideration in the field.

Effective Horizon and Model Accuracy The study in Jiang et al. (2015) investigates the impact of the horizon on planning under an inaccurate transition model, showing that a shorter horizon reduces the planning loss when the transition function is prone to estimation errors. However, applying its theoretical result to the case of reward function estimation is complicated due to the inherent complexity of IRL. There are two main challenges in examining the horizon’s role in IRL. First, the transition model estimation in Jiang et al. (2015) is conducted locally using state-action-state tuples for each state, allowing for a straightforward expression of estimation error by counting local samples. In contrast, the reward function estimation error relies heavily on the planning horizon, as IRL learns the reward function by matching the temporal behaviors with the expert. Second, planning with an estimated transition function in Jiang et al. (2015) is a single forward process, while IRL requires interdependent and iterative policy optimization and reward function estimation until convergence. This iterative process adds complexity to measuring the final policy performance. Despite these challenges, we aim to explore the effective horizon’s role in IRL, as it is vital for a more realistic IRL formulation and has the potential to further enhance the policy performance.

3 Problem formulation

In this work, we use *horizon* and *discount factor* interchangeably, as the discount factor implicitly incorporates the planning horizon by discounting future rewards. We consider an MDP (S, A, P, R_0, γ_0) , where S and A represent the state and action spaces, respectively. The transition function is denoted by $P : S \times A \times S \rightarrow [0, 1]$, and the ground-truth reward function is $R_0 : S \times A \rightarrow [0, R_{max}]$. The discount factor, γ_0 , implicitly determines the value of future rewards at the current time step. The optimal policy, π_{R_0, γ_0}^* , maximizes the total discounted reward based on

R_0 and γ_0 . The MDP is assumed to be ergodic, such that any state is reachable from any other state by following a suitable policy. In our setting, we are given the MDP without the reward function R_0 or the discount factor γ_0 . Instead, we have a set of expert demonstrations $D = \{\tau_0, \tau_1, \dots\}$, with each trajectory $\tau = (s_0, a_0, s_1, \dots, s_T)$ sampled from π_{R_0, γ_0}^* . We assume the expert policy is deterministic, hence observing a single (s, a) pair eliminates the policy estimation error for that state.

We propose to jointly learn the reward function and discount factor $(\hat{R}, \hat{\gamma})$ from limited expert demonstrations. The scarcity of data suggests that $(\hat{R}, \hat{\gamma})$ is susceptible to approximation errors, which consequently affects the induced optimal policy $\pi_{\hat{R}, \hat{\gamma}}^*$. We measure the quality of the $(\hat{R}, \hat{\gamma})$ pair by comparing the performance of its induced policy $\pi_{\hat{R}, \hat{\gamma}}^*$ with that of the ground-truth optimal policy π_{R_0, γ_0}^* , both evaluated under the ground-truth (R_0, γ_0) for fair comparison. Formally, we define the loss as the performance difference between the induced and ground-truth optimal policies:

$\left\| V_{R_0, \gamma_0}^{\pi_{R_0, \gamma_0}^*} - V_{R_0, \gamma_0}^{\pi_{\hat{R}, \hat{\gamma}}^*} \right\|_{\infty}$, where $V_{R, \gamma}^{\pi}$ represents the value function of policy π evaluated under (R, γ) . The ‘‘best’’ policy $\pi_{\hat{R}, \hat{\gamma}}^*$ is the one that minimizes this loss. We aim to use this loss to guide our

selection of the $(\hat{R}, \hat{\gamma})$ pair. The existing IRL works either use ground-truth γ_0 , or a smaller one to reduce the computation burden. In this work, we investigate when $\hat{\gamma} \leq \gamma_0$, how to choose the effective horizon that minimizes the loss defined above. We define the optimal horizon as:

$$\hat{\gamma}^* = \arg \min_{0 \leq \hat{\gamma} \leq \gamma_0} \left\| V_{R_0, \gamma_0}^{\pi_{R_0, \gamma_0}^*} - V_{R_0, \gamma_0}^{\pi_{\hat{R}, \hat{\gamma}}^*} \right\|_{\infty}. \quad (1)$$

4 Analysis

4.1 Overview

How does effective horizon affect reward learning from expert demonstrations? We formally analyze the dependency between the effective horizon and the quality of the learned reward function in different coverage of the expert data. Our main Theorem 4.1 shows that, given limited expert data coverage, employing a discount factor smaller than the ground-truth value allows IRL methods to learn ‘‘better’’ reward functions that induce policies more closely aligned with the expert.

Theorem 4.1. *Assume two MDPs with shared controlled Markov process: (S, A, P, R_0, γ_0) and $(S, A, P, \hat{R}, \hat{\gamma})$, whereas R_0 and γ_0 are the non-negative ground-truth reward function and the discount factor, while the reward function $\hat{R} : S \times A \rightarrow \mathbb{R}_{\geq 0}$ and the effective horizon $\hat{\gamma}$ are estimated from expert demonstrations visiting N states. Let $|\Pi_{\hat{\gamma}}|$ measure the complexity of the policy class induced by the estimated effective horizon $\hat{\gamma}$. Then, for the optimal policies π_{R_0, γ_0}^* induced by the ground-truth (R_0, γ_0) pair and $\pi_{\hat{R}, \hat{\gamma}}^*$ induced by the estimated $(\hat{R}, \hat{\gamma})$ pair, the difference in value function is bounded by:*

$$\left\| V_{R_0, \gamma_0}^{\pi_{R_0, \gamma_0}^*} - V_{R_0, \gamma_0}^{\pi_{\hat{R}, \hat{\gamma}}^*} \right\|_{\infty} \leq \frac{\gamma_0 - \hat{\gamma}}{(1 - \gamma_0)(1 - \hat{\gamma})} R_{max} + \frac{2R_{max}}{(1 - \hat{\gamma})^2} \sqrt{\frac{1}{2N} \log \frac{|S| |\Pi_{\hat{\gamma}}|}{2\delta}} \quad (2)$$

with probability at least $1 - \delta$.

Intuitively, Theorem 4.1 bounds the performance disparity between the policy induced by the learned $(\hat{R}, \hat{\gamma})$ and the expert policy as a sum of two terms: when $\hat{\gamma}$ increases, the first error term diminishes to encourage fidelity to the ground-truth γ_0 and approaches 0 when $\hat{\gamma} \rightarrow \gamma_0$, while the second error term grows due to overfitting arising from estimating a policy from an increasingly complex class $\Pi_{\hat{\gamma}}$ using the limited expert data covering N states. Consequently, these opposing error terms imply that an intermediate value of $\hat{\gamma}$ yields a better reward function that induces the most expert-like policy.

Let’s outline the proof idea below. We begin by establishing a bound on the estimation error of the reward function in terms of the *effective horizon* $\hat{\gamma}$ and the *expert state coverage* N , which corresponds to the second error term in the RHS of the overall bound in Theorem 4.1. To start with, the expert policy estimation error depends on both the expert state coverage N and the complexity of the policy class $\Pi_{\hat{\gamma}}$ used for estimation, while this complexity $|\Pi_{\hat{\gamma}}|$ in turn increases monotonically with the effective horizon $\hat{\gamma}$ (Theorem 4.3). As $\hat{\gamma}$ increases, the complexity of policy class $\Pi_{\hat{\gamma}}$ rises,

hence the fitted policy is more likely to overfit given limited expert state coverage N . Moreover, as IRL learns the reward function by matching the induced policy with the expert, the expert policy estimation error further propagates to the reward function estimation (Theorem 4.6). Therefore, the estimation error of the reward function in the second error term of Theorem 4.1 is bounded by i) the *effective horizon* $\hat{\gamma}$ that controls the complexity $|\Pi_{\hat{\gamma}}|$ of the induced policy class, and ii) the *expert state coverage* N .

Next, we derive the overall bound in Theorem 4.1. This bound measures the performance disparity between the policy induced by the learned reward-horizon pair and the optimal policy. Intuitively, this performance gap is caused by i) the difference in the horizons they optimize over, and ii) the difference in the reward functions. We, therefore, split this difference into two simpler error terms: i) the first term measures the performance drop due to evaluating the ground-truth optimal policy using different *horizons*, and ii) the second term accounts for the difference between the learned and ground-truth *reward functions*. This intermediate result is formalized in Theorem 4.7. Its first term can easily be simplified to the final form, while the estimation error of the *reward function* in the second term can be further bounded using the *effective horizon* and the *state coverage the expert samples*, as we have described above. This completes the proof.

The remainder of this section is organized as follows. In Section 4.2 we derive how the horizon controls the complexity measure of the policy class and prove the monotonicity (Theorem 4.3). In Section 4.3, we describe the feasible reward function set as a function of the expert policy (Lemma 4.5). In Section 4.4, we derive the error bound in reward function estimation from limited expert data coverage (Theorem 4.6). In Section 4.5, we prove how the error in reward function estimation and the difference in horizons propagate to the error in the value function estimation (Theorem 4.7). Finally, in Section 4.6, we combine all the results above and prove the final bound in Theorem 4.1.

4.2 Complexity of the Policy Class

We propose to use the number of potentially optimal policies under the fixed state space, action space, and transition function as the complexity measure of the policy class for different γ s under unknown reward function under mild conditions.

Definition 4.2 (Complexity Measure). The complexity measure of the policy class under a specific γ is defined as the number of optimal policies under the fixed state space S , action space A , and transition function P , but with arbitrary reward function $R' \in F_R$ that satisfies our assumption described later. Formally, we define the class of optimal policy corresponding to the given γ as:

$$\Pi_\gamma = \{\pi : \exists R \in F_R \text{ s.t. } \pi \text{ is optimal in } (S, A, P, R, \gamma)\},$$

where F_R is the set of reward functions that satisfy the following assumption: for each state $s \in S$, there exists a fixed state-action pair whose reward is strictly higher than any other actions, and R uniquely maximizes that state-action pair $R(s, a^*)$ for all states. To ensure a meaningful discussion, we assume a specific form for reward functions, as any policy can be optimal when considering arbitrary reward functions. The complexity of the policy class w.r.t γ is the number of optimal policies in the corresponding policy class, which is $|\Pi_\gamma|$.

Next, we prove that the complexity of the policy class defined in Definition 4.2 increases monotonically as the discount factor $\hat{\gamma}$ increases. We refer the readers to Appendix A for the full proof.

Theorem 4.3. *Under a specific MDP $M = (S, A, P, \cdot, \cdot)$ with fixed state space S , action space A , and transition function P , we define the optimal policy class according to Definition 4.2, then we have the following claims:*

1. $\forall \gamma, \gamma' \in [0, 1)$, if $\gamma < \gamma'$, then $\Pi_\gamma \subseteq \Pi_{\gamma'}$.
2. When $\gamma = 0$, $|\Pi_0| = 1$.
3. If $\gamma \rightarrow 1$, $|\Pi_\gamma| \geq (|A| - 1)^{|S|-1} |S|$ under mild conditions.

Intuitively, claim 1 asserts that as the discount factor γ grows, the number of potentially optimal policies increases monotonically. Claim 2 and 3 collectively demonstrate that, under mild conditions, policy complexity drastically rises with γ : when the discount factor is at its lowest ($\gamma = 0$), there is only one optimal policy, as the reward function has a unique maximum state-action pair for each state; while as γ increases, the optimal policy class can encompass nearly all possible policies, with $|\Pi_\gamma| = (|A| - 1)^{|S|-1} |S|$. In essence, γ effectively controls the complexity of the policy class.

4.3 Feasible Reward Function Set

In this section, we explicitly define all reward(s) that are consistent with the expert demonstration. To establish an algorithm-agnostic mapping from the fixed set of expert data and the effective horizon to the learned reward functions, we draw inspiration from Metelli et al. (2021) and define a reward function feasible set based on the fundamental formulation of IRL (Ng & Russell, 2000). In particular, the reward function feasible set includes all the reward functions whose induced policies match the expert data. Under this definition, we derive the explicit characterization of the reward feasible set as a function of the expert policy.

First, we implicitly define the feasible result set based on the IRL definition Ng & Russell (2000), adapting for the flexible discount factor.

Definition 4.4 (IRL Problem). Let $\mathcal{M} = (S, A, P)$ be the MDP without the reward function or discount factor. An IRL problem, denoted as $\mathfrak{R} = (\mathcal{M}, \pi^E)$, consists of the MDP and an expert's policy π^E . A reward $\hat{R} \in \mathbb{R}^{S \times A}$ is feasible for \mathfrak{R} if there exists a $\hat{\gamma}$ such that π^E is optimal for the MDP $\mathcal{M} \cup (\hat{R}, \hat{\gamma})$, i.e., $\pi^E \in \Pi_{\hat{R}, \hat{\gamma}}^*$. We use $\mathcal{R}_{\mathfrak{R}}$ to denote the set of feasible rewards for \mathfrak{R} .

To ensure \hat{R} and $\hat{\gamma}$ belong to the expert's feasible set π^E , two conditions derived from the advantage function $A_{\hat{R}, \hat{\gamma}}^{\pi^E}(s, a) = Q_{\hat{R}, \hat{\gamma}}^{\pi^E}(s, a) - V_{\hat{R}, \hat{\gamma}}^{\pi^E}(s)$ must be met: (1) if $\pi^E(a|s) > 0$, then $A_{\hat{R}, \hat{\gamma}}^{\pi^E}(s, a) = 0$; and (2) if $\pi^E(a|s) = 0$, then $A_{\hat{R}, \hat{\gamma}}^{\pi^E}(s, a) \leq 0$. The first condition ensures the expert's chosen actions have zero advantage, eliminating motivation to choose alternatives, while the second guarantees unchosen actions have non-positive advantages.

To explicitly express the feasible reward set, we introduce two operators: $(B^\pi g)(s, a) = g(s, a)\mathbb{1}\{\pi(a|s) > 0\}$ and $(\bar{B}^\pi g)(s, a) = g(s, a)\mathbb{1}\{\pi(a|s) = 0\}$ for any given policy π . The *expert-filter* $(B^\pi g)(s, a)$ retains $g(s, a)$ values for actions taken by the expert policy $\pi^E(a|s)$. Conversely, the *expert-filter-complement* $(\bar{B}^\pi g)(s, a)$ preserves values for actions not taken by the expert. The feasible reward set is derived as follows. The detailed derivation is provided in Appendix B.1.

Lemma 4.5 (Feasible Reward Set, adapted from Metelli et al. (2021)). *Let $\mathfrak{R} = (\mathcal{M}, \pi^E)$ be an IRL problem. Let $\hat{R} \in \mathbb{R}^{S \times A}$ and $0 < \hat{\gamma} < 1$, then \hat{R} is a feasible reward, i.e., $\hat{R} \in \mathcal{R}_{\mathfrak{R}}$ if and only if there exists $\zeta \in \mathbb{R}_{\geq 0}^{S \times A}$ and $V \in \mathbb{R}^S$ such that:*

$$\hat{R} = -\bar{B}^{\pi^E} \zeta + (E - \hat{\gamma}P)V, \quad (3)$$

whereas $E : \mathbb{R}^{|S|} \rightarrow \mathbb{R}^{|S| \times |A|}$ such that $(Ef)(s, a) = f(s)$.

The reward function in Lemma 4.5 comprises two terms based on the expert policy π^E and the MDP. Specifically, the first term $-\bar{B}^{\pi^E} \zeta$ depends solely on π^E : using *expert-filter-complement* on the non-negative function ζ , actions played by the expert (i.e., $\pi^E(a|s) > 0$) become zero, while unplayed actions (i.e., $\pi^E(a|s) = 0$) have non-positive values. The second term represents the policy's temporal effect, relying on the MDP's transition function. This can be viewed as reward-shaping via the value function, which preserves the expert policy's optimality.

4.4 Reward Inaccuracy due to the Estimation Error of Expert Policy

This section examines how the expert policy estimation error propagates to the feasible reward set estimation. We consider two IRL problems, $\mathfrak{R} = (\mathcal{M}, \pi^E)$ and $\hat{\mathfrak{R}} = (\mathcal{M}, \hat{\pi}^E)$, which differ only in expert policies: \mathfrak{R} utilizes the ground-truth expert policy, while $\hat{\mathfrak{R}}$ employs an estimated policy from samples. Since an IRL algorithm aligns its induced policy with the estimated expert policy, its feasible sets will be equivalent to that of the estimated expert policy. Intuitively, inaccuracies in estimating the expert policy π^E lead to errors in estimating the feasible sets $\mathcal{R}_{\mathfrak{R}}$. Our goal is to obtain a reward function \hat{R} with a feasible set "close" to R_0 's feasible set. Specifically, "closeness" is determined by the distance between the nearest reward functions in each set. The estimated $\mathcal{R}_{\hat{\mathfrak{R}}}$ is considered close to the exact $\mathcal{R}_{\mathfrak{R}}$ if, for every reward $R_0 \in \mathcal{R}_{\mathfrak{R}}$, there exists an estimated reward $\hat{R} \in \mathcal{R}_{\hat{\mathfrak{R}}}$ with a small $|R_0 - \hat{R}|$ value. The subsequent section outlines how errors in the expert policy π^E propagate to the reward functions.

Theorem 4.6 (Adapted from Theorem 3.1 in Metelli et al. (2021)). *Let $\mathfrak{R} = (\mathcal{M}, \pi^E)$ and $\hat{\mathfrak{R}} = (\mathcal{M}, \hat{\pi}^E)$ be two IRL problems. Then for any $R_0 \in \mathcal{R}_{\mathfrak{R}}$ such that $R_0 = -\bar{B}^{\pi^E} \zeta + (E - \gamma_0 P)V$ and*

$\|R_0\|_\infty \leq R_{\max}$ there exists $\widehat{R} \in \mathcal{R}_{\widehat{\gamma}}$ such that element-wise it holds that:

$$\left| R_0 - \widehat{R} \right| \leq \bar{B}^{\pi^E} B^{\widehat{\pi}^E} \zeta. \quad (4)$$

Furthermore, $\|\zeta\|_\infty \leq \frac{R_{\max}}{1-\gamma_0}$.

Intuitively, this result states the existence of a reward function \widehat{R} in the estimated feasible set $\mathcal{R}_{\widehat{\gamma}}$ which is bounded by the error in expert policy estimation. Specifically, this term is non-zero only for state-action pairs where $\pi^E(a|s) = 0$ and $\widehat{\pi}^E(a|s) > 0$, i.e., actions not taken by the expert but erroneously believed to be taken by the estimated expert policy. Thus, to zero out more entries in the reward function's error term, we need expert data to cover more states. We refer the readers to Appendix B.2 for the detailed proof.

4.5 Decomposing the Error in Value Function

This section decomposes the difference in value function between the two optimal policies induced by different reward-horizon into two simpler error terms: the first only depends on the difference in the horizon used for evaluating the ground-truth optimal policy, while the second term exclusively captures the estimation error of the reward function. Let $\pi_{R_0, \gamma_0}^* \in \Pi_{\gamma_0}$ be the optimal policy induced by the ground-truth reward and discounted factor, and $\pi_{\widehat{R}, \widehat{\gamma}}^* \in \Pi_{\widehat{\gamma}}$ be the optimal policy induced by the learned reward function and the corresponding $\widehat{\gamma}$. We aim to find an upper bound for the difference between the value functions of π_{R_0, γ_0}^* and $\pi_{\widehat{R}, \widehat{\gamma}}^*$ when evaluated under the ground-truth R_0 and γ_0 . As directly evaluating this error is challenging, we divide it into two more manageable error terms. In particular, we bound $\left\| V_{R_0, \gamma_0}^{\pi_{R_0, \gamma_0}^*} - V_{R_0, \gamma_0}^{\pi_{\widehat{R}, \widehat{\gamma}}^*} \right\|$ in terms of $\widehat{\gamma}$ and the difference in reward functions $\|R_0 - \widehat{R}\|$.

Theorem 4.7. *Assume two partial MDPs with shared $\mathcal{M} = (S, A, P)$. Let R_0 and γ_0 be the non-negative ground-truth reward function and the discounted factor of the exact MDP, while $\widehat{R} \in \mathbb{R}_{>0}^{S \times A}$ and $\widehat{\gamma}$ from the second MDP are estimated from data. Then, for the optimal policies π_{R_0, γ_0}^* induced by the ground-truth (R_0, γ_0) pair and $\pi_{\widehat{R}, \widehat{\gamma}}^*$ induced by the estimated $(\widehat{R}, \widehat{\gamma})$ pair, the difference in value function is bounded below:*

$$\left\| V_{R_0, \gamma_0}^{\pi_{R_0, \gamma_0}^*} - V_{R_0, \gamma_0}^{\pi_{\widehat{R}, \widehat{\gamma}}^*} \right\| \leq \frac{\gamma_0 - \widehat{\gamma}}{(1-\gamma_0)(1-\widehat{\gamma})} R_{\max} + \frac{2}{1-\widehat{\gamma}} \|R_0 - \widehat{R}\|. \quad (5)$$

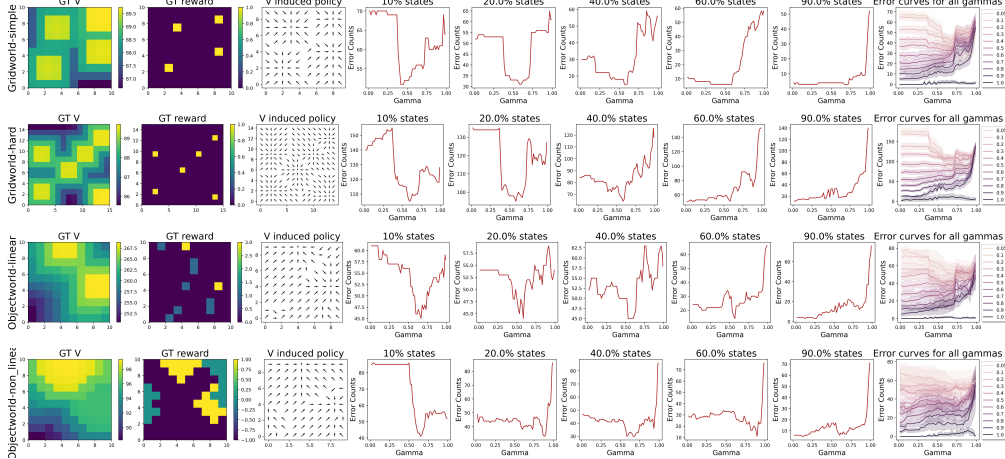
The proof for Theorem 4.7 can be found in Appendix B.3. The overall error in Theorem 4.7 consists of two terms. The first error term represents the performance loss due to utilizing a smaller discount factor, $\widehat{\gamma} < \gamma_0$. As $\widehat{\gamma}$ increases, this error decreases and approaches 0 when $\widehat{\gamma} \rightarrow \gamma_0$. The second error term arises from employing the learned reward function, \widehat{R} , instead of the ground-truth reward function, R_0 . Notably, \widehat{R} is learned using a reduced $\widehat{\gamma}$ from limited expert demonstrations. Contrary to the first error term, the second error increases with larger γ_0 values, as the reward function estimation error is compounded over an extended horizon, leading to a greater overall loss. Since the two error terms in the RHS of Theorem 4.7 are influenced by γ_0 in opposite ways, the bound will be optimized at an intermediate value.

4.6 Overall Bound on the Performance Loss

We have established i) how the effective horizon controls the complexity of the induced policy class (Theorem 4.3), ii) how the expert policy estimation error bounds the reward-horizon estimation (Theorem 4.6), and iii) how to decompose the performance gap between the induced and ground-truth optimal policies (Theorem 4.7). In this section, we integrate these results to prove how would the effective horizon affects the performance of final policy induced by the learned reward function from limited expert state coverage.

We first deduce how the effective horizon affects expert policy estimation error in cases of limited expert state coverage. As demonstrated in Theorem 4.3, policy class complexity increases monotonically with the effective horizon. Utilizing Hoeffding's inequality, we bound the expert policy

Table 1: Summary of LP-IRL with varying discount factors across four tasks. The *error counts* measure the number of actions in a policy that deviate from the expert’s actions. Each task displays the ground-truth value function (column 1), reward function (column 2), expert policy (column 3), error count curves for different expert data coverage in a **single instance** (columns 4-8), and error curve summary for a **batch** of 10 MDPs (column 9). In all four tasks, $\gamma_0 = 0.99$. The optimal discount factor $\hat{\gamma}^* < \gamma_0$ for varying expert data coverage. MaxEnt-IRL has similar curves in Table 2.



estimation error by the policy class complexity based on i.i.d expert samples covering N states. The resulting inequality indicates that a smaller horizon can control policy class complexity and reduce overfitting in expert policy estimation when expert state coverage is limited. For a detailed proof, please refer to Appendix B.4.

Finally, we substitute the bound on the estimation error of the expert policy to derive an upper bound on the reward function estimation error in Theorem 4.7, completing the proof in Theorem 4.1. The overall loss comprises two terms that exhibit opposing dependencies on $\hat{\gamma}$. This suggests the existence of an intermediate value $0 < \hat{\gamma} < \gamma_0$ that minimizes the overall loss, which will be empirically demonstrated in the following section.

5 Experiments

In this section, we empirically examine Theorem 4.1 using both linear programming IRL (LP-IRL) (Ng & Russell, 2000) and maximum entropy IRL (MaxEnt-IRL) (Ziebart et al., 2008) adapted for partial expert coverage and varying discount factors setting (implementation details in Appendix D and E respectively). Both of the algorithms originally utilize the ground-truth discount factor, γ_0 , to learn reward functions. To extend from their original settings to jointly learn the proposed function class $(\hat{R}, \hat{\gamma})$, we apply a cross-validation extension to optimize the discount factor in the modified IRL methods (details in section 5.2). Specifically, we answer the following questions:

- Q.1 Can a lower $\hat{\gamma} < \gamma_0$ improve IRL policy performance?
- Q.2 How does $\hat{\gamma}^*$ change with increasing expert coverage N ?
- Q.3 Is the cross-validation extension effective in finding $\hat{\gamma}^*$?

We evaluate the performance of LP-IRL and MaxEnt-IRL on four Gridworld and Objectworld tasks with varying reward complexity. For Q.1, we measure the number of incorrectly induced actions under varying discounted factors and different coverage of expert data. Our findings show that the optimal $\hat{\gamma}$ s across all expert coverage are smaller than γ_0 for both algorithms. For Q.2, we plot how the optimal discount factors change as the expert coverage increases. The consistent U-shaped curves observed in all cases align with the anticipated overfitting effect implied by the second error term in Equation 2. For Q.3, we compare the performance of policies selected via cross-validation with the baseline policies selected using the oracle counts of incorrect actions (this baseline “cheats” by learning the reward function using 100% of the expert data and validating using the error counts in

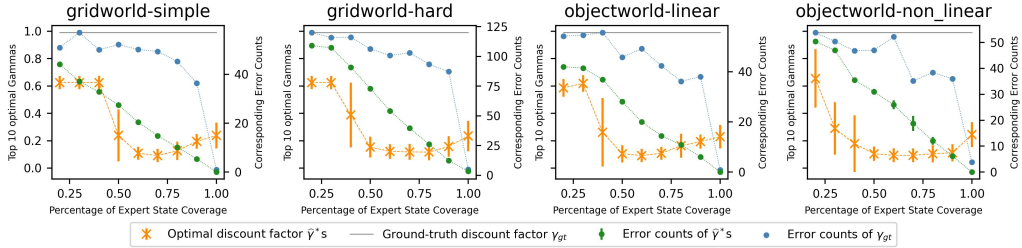


Figure 1: Optimal gammas ($\hat{\gamma}^*$) for LP-IRL at different expert demonstration coverages. Top 10 $\hat{\gamma}^*$ s are obtained using the algorithm in Section 5.2. Orange curves show how $\hat{\gamma}^*$ changes with expert coverage, while green curves display corresponding error counts. Ground-truth $\gamma_0 = 0.99$ is depicted in grey, with corresponding error lines in blue. As expert coverage increases, $\hat{\gamma}^*$ drastically decreases before gently increasing for all four tasks, indicating overfitting is prominent with scarce expert data.

the unseen states). Our results indicate that the discrepancy in performance is negligible for all tasks, demonstrating the effectiveness of cross-validation in selecting $\hat{\gamma}^*$.

5.1 Task Setup

We design four tasks of varying complexity in reward functions: Gridworld-simple, Gridworld-hard, Objectworld-linear, and Objectworld-nonlinear, adapted from Ng & Russell (2000) and Levine et al. (2011). We illustrate each task instance in the first three columns of Tables 1 and more details on the task specification are in Appendix C. The ground-truth discount factor is $\gamma_0 = 0.99$.

The Gridworld tasks provide sparse rewards only at randomly sampled goals: Gridworld-simple has fewer goals (4) and a smaller state space (10×10 states), while Gridworld-hard has more goals (6) and a larger state space (15×15 states). On the other hand, the Objectworld tasks have denser ground-truth rewards that are functions of nearby object features. The reward function for Objectworld-linear is linear with respect to the features of nearby objects, while that of Objectworld-nonlinear is non-linear. Intuitively, learning a complex reward function may be more susceptible to overfitting, especially when expert state coverage is sparse compared to the state space.

We consider different percentages of state coverage by expert demonstrations. We say a set of expert demonstrations $D = \{\tau_0, \tau_1, \dots\}$ covers a set of N states, with the set being the union of states traversed by trajectories in D . A demonstration set D covers $K\%$ of states if $K\% = N/|S|$, with S denoting the state space. We evaluate induced policy performance by *counting errors in state sets*: the number of states where induced and expert policies execute different actions.

5.2 Cross Validation Extension

We use cross-validation to determine the optimal discount factor $\hat{\gamma}^*$, given the expert demonstrations D covering N states. We divide D into training and validation sets, ensuring no overlap. Next, we uniformly sample M discount factors from $(0, \gamma_0)$, learning the reward function R_γ for each using the training set. The optimal reward-horizon pair minimizes error count in the validation set. We randomly sample 10 environments per task, reporting mean and standard deviation errors. For all tasks, we assign 80% of demonstration as the training set and 20% as the validation set. To better understand the effectiveness of cross-validation, we employ an oracle representing the best policy learnable from the available expert data. This oracle, considered “cheating”, utilizes the entire state space (both observed and unobserved states) for validation and leverages all expert data for training. We examine whether the $\hat{\gamma}^*$ s chosen by cross-validation correspond to this oracle.

5.3 Results

We assess the impact of the *effective horizon* on IRL by examining both LP-IRL and MaxEnt-IRL across four tasks.¹ The policy performance results are presented in Tables 1 and 2 for LP-IRL and MaxEnt-IRL, respectively. We utilize the *error counts* metric, which quantifies the discrepancies between induced and expert policies by counting differing actions in corresponding states.

Q.1 Optimal Discount Factor is Lower than Ground-Truth.

¹LP-IRL utilizes a discount factor γ , while MaxEnt-IRL employs a horizon T . To ease the presentation, our analysis treats γ and T interchangeably, with findings for γ also applicable to T , unless specified otherwise.

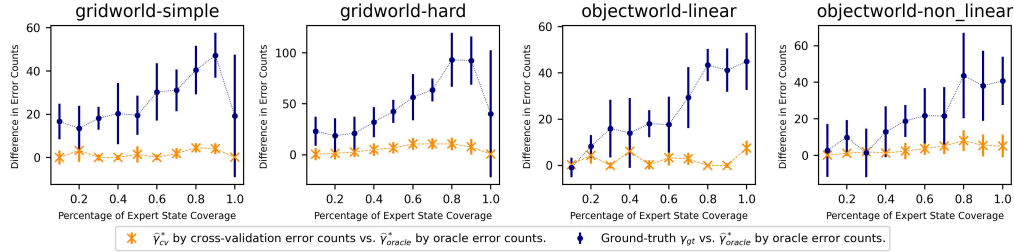


Figure 2: Cross-validation results for the four tasks in LP-IRL. The x -axis represents expert data coverage, while the y -axis shows error count differences in all states for various $\hat{\gamma}^*$ s: $\hat{\gamma}_{cv}^*$ learned via cross-validation, and $\hat{\gamma}_{oracle}^*$ chosen optimally using the oracle. Orange dots depict error count differences between the induced policies of $\hat{\gamma}_{cv}^*$ and $\hat{\gamma}_{oracle}^*$, while blue dots represent differences between the induced policies of γ_0 and $\hat{\gamma}_{oracle}^*$.

As illustrated in Tables 1 and 2, the optimal discount factor $\hat{\gamma}^* < \gamma_0$ for all four tasks across various expert data coverage in both LP-IRL and MaxEnt-IRL. For low coverage, the error count curves are generally U-shaped: discrepancies with the expert policy decrease as $\hat{\gamma}$ increases to the “sweet spot” and then rise drastically. This confirms our error bounds in Theorem 4.1: with small $\hat{\gamma}$, the second error term in Equation 2 caused by overfitting is less prominent, and increasing $\hat{\gamma}$ allows temporal extrapolation, reducing the overall error. However, with larger $\hat{\gamma}$, overfitting becomes more significant, outweighing the reduction in the first error term and increasing the overall error.

Under high data coverage, error counts either remain low (in LP-IRL) or drops initially (in MaxEnt-IRL) for small $\hat{\gamma}$ and strictly increase as $\hat{\gamma}$ grows further for both methods, implying that $\hat{\gamma}^* < \gamma_0$ induces the most expert-like policy, confirming our theoretical result. Interestingly, for LP-IRL, the error counts do not initially drop as $\hat{\gamma}$ increases. This is due to accurate step-wise behavior matching under dense expert data, making the performance gains from temporal reasoning (the first error term) negligible. This supports Spencer et al. (2021)’s insight that naive behavioral cloning excels with large expert demonstration coverage compared to IRL algorithms. However, this low error counts for small $\hat{\gamma}$ s are not seen in MaxEnt-IRL as it parameterizes the reward function linear in the state features, limiting its capability to precisely copy the step-wise actions even under high data coverage.

Q.2 Optimal Discount Factors Vary with Expert Data Coverage.

Figures 1 and 3 illustrate how the optimal discount factor $\hat{\gamma}^*$ changes with increasing expert coverage for LP-IRL and MaxEnt-IRL respectively. Under low data coverage, $\hat{\gamma}^*$ starts high, as temporal reasoning benefits outweigh overfitting harms. In essence, with very few samples, the estimation error of the expert policy remains high regardless of overfitting. A large $\hat{\gamma}^*$ enables extrapolation of actions for the nearby unobserved states, thereby reducing the first error term in Theorem 4.1 and enhancing overall error reduction. For moderate data coverage, $\hat{\gamma}^*$ decreases: despite the expert policy estimation improves with more data, the data coverage is still limited. Hence, the overall error bound favors a smaller $\hat{\gamma}^*$ to mitigate overfitting, reducing the second term’s error despite sacrificing some gains from the temporal reasoning. As coverage further increases, $\hat{\gamma}^*$ rises since overfitting is less of a concern, and larger values enable more temporal reasoning.

Overall, as expert coverage increases, error counts for $\hat{\gamma}^*$ strictly decrease and remain below those for γ_0 , indicating that $\hat{\gamma}^*$ allows IRL to learn more effectively from additional expert data.

Q.3 Cross-Validation Effectively Selects Optimal Discount Factors.

Figures 2 and 4 summarize the cross-validation results for LP-IRL and MaxEnt-IRL respectively. The discrepancy in the policy performance between $\hat{\gamma}_{cv}^*$ and $\hat{\gamma}_{oracle}^*$ (orange curves) is consistently near-zero for all four tasks, indicating that cross-validation error effectively approximates oracle error for choosing $\hat{\gamma}^*$. Additionally, blue curves, representing the extra error using γ_0 compared to $\hat{\gamma}_{oracle}^*$, are always higher than the orange curves, suggesting that $\hat{\gamma}_{cv}^*$ results in better-performing policies than the ground-truth γ_0 , confirming our Theorem 4.1.

6 Conclusion

In this paper, we present a theoretical analysis on IRL that unveils the potential of a reduced horizon in inducing a more expert-like policy, particularly in data-scarce situations. Our findings reveals an important insight on role of the horizon in IRL: it controls the complexity of the induced policy class, therefore reduces overfitting to the limited expert data. We, therefore, propose a more natural IRL

function class that jointly learns reward-horizon pairs and empirically substantiate our analysis using a cross-validation extension for the existing IRL algorithms. As overfitting remains a challenge for IRL, especially with scarce expert data, we believe our findings offer valuable insights for the IRL community on better IRL formulations.

References

- Abbeel, P. and Ng, A. Apprenticeship learning via inverse reinforcement learning. In *Proc. Int. Conf. on Machine Learning*, 2004.
- Boularias, A., Kober, J., and Peters, J. Relative entropy inverse reinforcement learning. In *Proc. Int. Conf. on Artificial Intelligence & Statistics*, 2011.
- Finn, C., Christiano, P., Abbeel, P., and Levine, S. A connection between generative adversarial networks, inverse reinforcement learning, and energy-based models. In *Advances in Neural Information Processing Systems*, 2016a.
- Finn, C., Levine, S., and Abbeel, P. Guided cost learning: Deep inverse optimal control via policy optimization. In *Proc. Int. Conf. on Machine Learning*, 2016b.
- Fu, J., Luo, K., and Levine, S. Learning robust rewards with adversarial inverse reinforcement learning. In *Proc. Int. Conf. on Learning Representations*, 2018.
- Ghasemipour, S. K. S., Zemel, R., and Gu, S. A divergence minimization perspective on imitation learning methods. In *Proc. Conference on Robot Learning*, 2019.
- Ho, J. and Ermon, S. Generative adversarial imitation learning. In *Advances in Neural Information Processing Systems*, 2016.
- Hoshino, H., Ota, K., Kanazaki, A., and Yokota, R. Opirl: Sample efficient off-policy inverse reinforcement learning via distribution matching. In *Proc. IEEE Int. Conf. on Robotics & Automation*, pp. 448–454, 2022. doi: 10.1109/ICRA46639.2022.9811660.
- Jiang, N., Kulesza, A., Singh, S., and Lewis, R. The dependence of effective planning horizon on model accuracy. In *Proc. Int. Conf. on Autonomous Agents & Multiagent Systems*, volume 2, pp. 1181–1189, 05 2015.
- Ke, L., Choudhury, S., Barnes, M., Sun, W., Lee, G., and Srinivasa, S. Imitation learning as f-divergence minimization. In *Algorithmic Foundations of Robotics XIV—Proc. Int. Workshop on the Algorithmic Foundations of Robotics (WAFR)*, 2020.
- Lee, K., Isele, D., Theodorou, E. A., and Bae, S. Spatiotemporal costmap inference for MPC via deep inverse reinforcement learning. In *IEEE Robotics & Automation Letters*, 2022. doi: 10.48550/ARXIV.2201.06539. URL <https://arxiv.org/abs/2201.06539>.
- Levine, S., Popovic, Z., and Koltun, V. Nonlinear inverse reinforcement learning with gaussian processes. In *Advances in Neural Information Processing Systems*, 12 2011.
- MacGlashan, J. and Littman, M. L. Between imitation and intention learning. In *Proc. Int. Jnt. Conf. on Artificial Intelligence*, 2015.
- Metelli, A. M., Ramponi, G., Concetti, A., and Restelli, M. Provably efficient learning of transferable rewards. In *Proc. Int. Conf. on Machine Learning*, 2021.
- Ng, A. Y. and Russell, S. J. Algorithms for inverse reinforcement learning. In *Proc. Int. Conf. on Machine Learning*, San Francisco, CA, USA, 2000. Morgan Kaufmann Publishers Inc. ISBN 1558607072.
- Ni, T., Sikchi, H., Wang, Y., Gupta, T., Lee, L., and Eysenbach, B. f-irl: Inverse reinforcement learning via state marginal matching. In *Proc. Conference on Robot Learning*, 11 2020.
- Osa, T., Pajarinen, J., Neumann, G., Bagnell, J. A., Abbeel, P., Peters, J., et al. An algorithmic perspective on imitation learning. *Foundations and Trends® in Robotics*, 7(1-2):1–179, 2018.

- Pirotta, M. and Restelli, M. Inverse reinforcement learning through policy gradient minimization. In *Proc. AAAI Conf. on Artificial Intelligence*, 2016.
- Ramachandran, D. and Amir, E. Bayesian inverse reinforcement learning. In *Proc. Int. Jnt. Conf. on Artificial Intelligence*, 2007.
- Ramponi, G., Drappo, G., and Restelli, M. Inverse reinforcement learning from a gradient-based learner. *Advances in Neural Information Processing Systems*, 33:2458–2468, 2020.
- Ratliff, N. D., Bagnell, J. A., and Zinkevich, M. A. Maximum margin planning. In *Proc. Int. Conf. on Machine Learning*, 2006.
- Spencer, J., Choudhury, S., Venkatraman, A., Ziebart, B. D., and Bagnell, J. A. Feedback in imitation learning: The three regimes of covariate shift. *ArXiv*, abs/2102.02872, 2021.
- Wulfmeier, M., Ondruska, P., and Posner, I. Maximum entropy deep inverse reinforcement learning. In *Advances in Neural Information Processing Systems*, 2016.
- Xu, Y., Gao, W., and Hsu, D. Receding horizon inverse reinforcement learning. In *Advances in Neural Information Processing Systems*, 2022.
- Ziebart, B. D., Maas, A., Bagnell, J. A., and Dey, A. K. Maximum entropy inverse reinforcement learning. In *Proc. AAAI Conf. on Artificial Intelligence*, 2008.

A Complexity Measure of Policy

Definition A.1 (Reward and Policy Equivalence). For an MDP $M = (S, A, P, \cdot, \gamma)$, we define two bounded reward functions R and R' to be equivalent, i.e. $R \equiv R'$, if and only if they induce the same set of optimal policies.

Lemma A.2 (Potential-based Reward Shaping). . For an MDP $M = (S, A, P, \cdot, \gamma)$, two bounded reward functions R and R' are equivalent, i.e. $R \equiv R'$, if and only if there exists a bounded potential function $\phi : S \rightarrow \mathbb{R}$ such that for all $s, s' \in S$ and $a \in A$:

$$R'(s, a, s') = R(s, a, s') + \gamma\phi(s') - \phi(s) \quad (6)$$

Remark. We extend lemma A.2 from $R(s, a, s')$ to $R(s, a)$. For an MDP $M = (S, A, P, \cdot, \gamma)$, two bounded reward functions $R(s, a)$ and $R'(s, a)$ are equivalent, if and only if there exists a bounded potential function $\phi : S \rightarrow \mathbb{R}$ such that for all $s, s' \in S$ and $a \in A$:

$$R'(s, a) = R(s, a) + \gamma \sum_{s'} P(s'|a, s)\phi(s') - \phi(s) \quad (7)$$

Proof. Consider the reward function $R(s, a, s')$, its $R(s, a)$ counterpart is defined as follows:

$$R(s, a) = \sum_{s'} P(s'|a, s)R(s, a, s') \quad (8)$$

Now, we consider $R'(s, a, s') \equiv R(s, a, s')$ by potential-based shaping with potential function ϕ , we have the following reward-equivalent shaping for $R'(s, a)$:

$$\begin{aligned} R'(s, a) &= \sum_{s'} P(s'|a, s)R'(s, a, s') \\ &= \sum_{s'} P(s'|a, s)(R(s, a, s') + \gamma\phi(s') - \phi(s)) \\ &= \sum_{s'} P(s'|a, s)R(s, a, s') + \gamma \sum_{s'} P(s'|a, s)\phi(s') - \phi(s) \sum_{s'} P(s'|a, s) \\ &= R(s, a) + \gamma \sum_{s'} P(s'|a, s)\phi(s') - \phi(s) \end{aligned} \quad (9)$$

□

Proof. Proof of theorem 1, claim 1. Given $\gamma, \gamma' \in [0, 1], \gamma < \gamma'$, we prove if $\pi \in \Pi_\gamma$, then $\pi \in \Pi_{\gamma'}$ as well. Formally, let π be the optimal policy in MDP $M = (S, A, P, R, \gamma)$, we construct a reward function $R' \in F_R$ such that π is still optimal in MDP (S, A, P, R', γ') .

Given policy π , let P^π be the transition function matrix of size $|S| \times |S|$ such that $[P^\pi](s, s') = P(s'|a(s), s)$, and R^π be the reward vector of size $|S|$ such that $[R^\pi](s) = R(s, \pi(s))$. We can write the value function $V_{R, \gamma}^\pi$ of policy π evaluated under the reward function R and discount factor γ as follows:

$$V_{R, \gamma}^\pi = R^\pi + \gamma P^\pi V_{R, \gamma}^\pi \quad (10)$$

Next, we apply a potential-based shaping to the original reward function R^π . Let R'^π be the shaped reward vector of size $|S|$ such that $[R'^\pi](s) = R'(s, \pi(s))$, we have:

$$R'^\pi = R^\pi + \gamma P^\pi \phi - \phi \quad (11)$$

where ϕ is the potential vector defined as follows:

$$\phi = \frac{\gamma' - \gamma}{\gamma} V_{R', \gamma}^\pi \quad (12)$$

With this shaped reward function R' and γ , we have the new value function:

$$\begin{aligned}
V_{R',\gamma}^\pi &= R'^\pi + \gamma P^\pi V_{R',\gamma}^\pi \\
&= R^\pi + \gamma P^\pi \phi - \phi + \gamma P^\pi V_{R',\gamma}^\pi \\
&= R^\pi + \gamma \frac{\gamma' - \gamma}{\gamma} P^\pi V_{R',\gamma}^\pi - \frac{\gamma' - \gamma}{\gamma} V_{R',\gamma}^\pi + \gamma P^\pi V_{R',\gamma}^\pi \\
&= R^\pi + \gamma' P^\pi V_{R',\gamma}^\pi - \frac{\gamma' - \gamma}{\gamma} V_{R',\gamma}^\pi
\end{aligned}$$

Rearranging, we have:

$$V_{R',\gamma}^\pi = (I - \gamma' P^\pi + \frac{\gamma' - \gamma}{\gamma})^{-1} R^\pi \quad (13)$$

Since $R \equiv R'$, their respective value function $V_{R,\gamma}^\pi$ and $V_{R',\gamma}^\pi$ induce the same set of optimal policies. We emphasize that R' is not necessary from F_R . To prove that any optimal policy $\pi \in \Pi_\gamma$ is still optimal in $\Pi_{\gamma'}$, we construct a $\hat{R} \in F_R$ which can make its value function $V_{\hat{R},\gamma'}^\pi$ evaluated with larger γ' the same as $V_{R',\gamma}^\pi$.

We construct \hat{R} as follows:

$$\hat{R}^\pi = R^\pi - \frac{\gamma' - \gamma}{\gamma} V_{R,\gamma'}^\pi \quad (14)$$

The value function $V_{\hat{R},\gamma'}^\pi$ for \hat{R} and γ' is:

$$V_{\hat{R},\gamma'}^\pi = \hat{R}^\pi + \gamma' P^\pi V_{\hat{R},\gamma'}^\pi \quad (15)$$

$$= R^\pi - \frac{\gamma' - \gamma}{\gamma} V_{R,\gamma'}^\pi + \gamma' P^\pi V_{\hat{R},\gamma'}^\pi \quad (16)$$

Rearrange, we have:

$$V_{\hat{R},\gamma'}^\pi = (I - \gamma' P^\pi + \frac{\gamma' - \gamma}{\gamma})^{-1} R^\pi \quad (17)$$

$$= V_{R',\gamma}^\pi \quad (18)$$

It suffices to show that the construction for \hat{R} in equation (14) satisfies $\hat{R} \in F_R$. We now write the construction for $\hat{R}(s, a)$ for every (s, a) pair:

$$\hat{R}(s, a) = R(s, a) - \frac{\gamma' - \gamma}{\gamma} V_{R,\gamma'}^\pi(s) \quad (19)$$

We notice that the second term is a factor of the value function, which only depends on the current state s . Therefore, $R(s, a^*) > R(s, a)$ iff $\hat{R}(s, a^*) > \hat{R}(s, a)$ for all $s \in S$. That is, $\hat{R} \in F_R$. \square

Proof. Proof of theorem 1, claim 2. $\gamma = 0$ is the special case where the planning only performs one-step look ahead and optimize the immediate reward greedily. When $\gamma = 0$, the planning objective reduces to

$$\pi_{R,\gamma=0}^* = \arg \max_{\pi \in \Pi} \mathbb{E}_{a_t \sim \pi(s_t)} [R(s_t, a_t)] \quad (20)$$

Given the assumption that $\forall s \in S$, $\arg \max_{a \in A} R(s, a)$ is unique, then π^* is also unique and $|\Pi_0| = 1$. \square

Proof. Proof of theorem 1, claim 3. This proof is by construction. We consider a fully connected state space with the transition function $P(s'|s, a)$ defined below. Recall that for each $s \in S$, there exists a unique a_s^* that maximizes $R(s, a)$, we first define the transition for each state for taking this a_s^* :

$$\forall s \in S, P(s'|s, a_s^*) = \begin{cases} 1 & \text{if } s' = s \\ 0 & \text{otherwise} \end{cases} \quad (21)$$

For all other actions $a \in A/\{a_s^*\}$ in state $s \in S$, the transition function is defined as follows:

$$P(s'|s, a) = \frac{1}{|S|-1}, \forall s' \in S/\{s\} \quad (22)$$

The given transition model corresponds to a fully connected state space where (s, a_s^*) creates a self-loop, and any other action has an equal probability of transitioning to different states. We construct $R_{s^*} \in F_R$ in this manner: for a state $s^* \in S$, let $R_{s^*}(s^*, a_{s^*}^*) > 2|S|R_{s^*}(s, a_s^*)$ for any other state $s \in S/\{s^*\}$. Consider an arbitrary policy π with the constraints $\pi(s^*) = a_{s^*}^*$ and $\pi(s) \neq a_s^*$ for other states. We demonstrate that this policy π is optimal in R_{s^*} and P . The optimality of π at s^* is apparent since this state is absorbing and π selects the action maximizing immediate reward. For any other state s , we show that π is optimal by calculating the optimal Q-value of $(s, \pi(s))$ compared to any other action a . Remember that for $s \neq s^*$, we constrain π not to choose a_s^* , so the alternative choice of a is to precisely select a_s^* . Therefore, we have:

$$Q^*(s, \pi(s)) = R(s, \pi(s)) + \gamma \left(\frac{1}{|S|-1} \frac{1}{1-\gamma} R(s^*, a_{s^*}^*) + \frac{1}{|S|-1} \sum_{s' \in S/\{s^*\}} Q(s', \pi(s')) \right) \quad (23)$$

$$Q^*(s, a_s^*) = R(s, a_s^*) + \frac{\gamma}{1-\gamma} R(s, a_s^*) \quad (24)$$

We have:

$$\begin{aligned} Q^*(s, \pi(s)) &> R(s, \pi(s)) + \frac{\gamma}{1-\gamma} \frac{1}{|S|-1} R(s^*, a_{s^*}^*) \\ &> R(s, \pi(s)) + \frac{\gamma}{1-\gamma} \frac{2|S|}{|S|-1} R(s, a_s^*) \\ &> R(s, \pi(s)) + \frac{\gamma}{1-\gamma} 2R(s, a_s^*) \end{aligned} \quad (25)$$

Since $2R(s, a_s^*) - R(s, a_s^*) = R(s, a_s^*) > 0$, and as γ approaches one, $\frac{\gamma}{1-\gamma}$ tends to infinity, so for sufficiently large γ we can guarantee that $Q^*(s, \pi(s)) \geq Q^*(s, a)$. Given each s^* and its corresponding R_{s^*} , under our constraints for π , there are $(|A|-1)^{|S|-1}$ such policies. In addition, since the choice of s^* is arbitrary, we can form $|S|$ of such R_{s^*} , therefore, the total number of such policy is $(|A|-1)^{|S|-1}|S|$. \square

B Proof for Section 4

B.1 Proof for Lemma 4.5

Proof. This proof is adapted from the proof of Lemma B.1 and Lemma 3.2 in Metelli et al. (2021). Recall that we use the advantage function to derive two conditions such that the expert policy π^E is optimal under the reward function \hat{R} and $\hat{\gamma}$. Specifically,

$$Q_{\hat{R}, \hat{\gamma}}^{\pi^E}(s, a) - V_{\hat{R}, \hat{\gamma}}^{\pi^E}(s) = 0 \quad \text{if } \pi^E(a|s) > 0, \quad (26)$$

$$Q_{\hat{R}, \hat{\gamma}}^{\pi^E}(s, a) - V_{\hat{R}, \hat{\gamma}}^{\pi^E}(s) \leq 0 \quad \text{if } \pi^E(a|s) = 0. \quad (27)$$

Consider an IRL problem $\mathfrak{R} = (\mathcal{M}, \pi^E)$. A Q-function satisfies the specified conditions if and only if there exist $\zeta \in \mathbb{R}_{\geq 0}^{S \times A}$ and $V \in \mathbb{R}^{|S|}$ such that:

$$Q_{\hat{R}, \hat{\gamma}} = -\bar{B}^{\pi^E} \zeta + EV. \quad (28)$$

Given that $\pi^E \bar{B}^{\pi^E} = \mathbf{0}_S$ and $\pi^E E = I_S$, the corresponding value function is $V_{\hat{R}, \hat{\gamma}} = \pi^E Q_{\hat{R}, \hat{\gamma}} = V$. For any $s \in S$ and $a \in A$ with $\pi^E(a|s) > 0$, we obtain $Q_{\hat{R}, \hat{\gamma}}(s, a) = V(s) = V_{\hat{R}, \hat{\gamma}}(s)$. This establishes the first condition in equation 26. If $a \in A$ has $\pi^E(a|s) = 0$, then $Q_{\hat{R}, \hat{\gamma}}(s, a) =$

$-\zeta(s, a) + V(s) = -\zeta(s, a) + V_{\widehat{R}, \widehat{\gamma}}(s) \leq V_{\widehat{R}, \widehat{\gamma}}(s)$. This verifies the second condition in equation 27. Conversely, if $Q_{\widehat{R}, \widehat{\gamma}}$ fulfills the two conditions, we set $V = V_{\widehat{R}, \widehat{\gamma}}$ and $\zeta = EV_{\widehat{R}, \widehat{\gamma}} - Q_{\widehat{R}, \widehat{\gamma}} \leq 0$.

Next, recall that $Q_{\widehat{R}, \widehat{\gamma}} = \widehat{R} + \widehat{\gamma}P\pi^E Q_{\widehat{R}, \widehat{\gamma}}$. The Q-function can be written as the fixed point of the above Bellman equation: $Q_{\widehat{R}, \widehat{\gamma}} = (I_{S \times A} - \widehat{\gamma}P\pi^E)^{-1}\widehat{R}$, and for $\widehat{\gamma} < 1$, the matrix is invertible. In other words, with fixed π^E , P , and $\widehat{\gamma} < 1$, there is a one-to-one correspondence between Q-functions and rewards. From equation 28, we obtain:

$$\begin{aligned}\widehat{R} &= (I_{S \times A} - \widehat{\gamma}P\pi^E)(-\bar{B}^{\pi^E}\zeta + EV) \\ &= -\bar{B}^{\pi^E}\zeta + \widehat{\gamma}P\pi^E\bar{B}^{\pi^E}\zeta + (E - \widehat{\gamma}P\pi^E)V \\ &= -\bar{B}^{\pi^E}\zeta + (E - \widehat{\gamma}P)V,\end{aligned}\tag{29}$$

since $\pi^E\bar{B}^{\pi^E} = \mathbf{0}_S$ and $\pi^EE = I_S$. \square

B.2 Proof for Theorem 4.6

Proof. This proof is adapted from Theorem 3.1 in Metelli et al. (2021). Note that R_0 in Theorem 4.6 is the ground-truth reward function and has the corresponding ground-truth discount factor γ_0 . Using Lemma 4.5, we express reward functions $R_0 \in \mathcal{R}_{\mathfrak{R}}$ and $\widehat{R} \in \mathcal{R}_{\widehat{\mathfrak{R}}}$ as:

$$R_0 = -\bar{B}^{\pi^E}\zeta + (E - \gamma_0P)V,\tag{30}$$

$$\widehat{R} = -\bar{B}^{\hat{\pi}^E}\hat{\zeta} + (E - \widehat{\gamma}P)\hat{V},\tag{31}$$

where $V, \hat{V} \in \mathbb{R}^S$ and $\zeta, \hat{\zeta} \in \mathbb{R}_{\geq 0}^{S \times A}$. To find the existence of $\widehat{R} \in \mathcal{R}_{\widehat{\mathfrak{R}}}$, we choose $\hat{V} = (E - \widehat{\gamma}P)^{-1}(E - \gamma_0P)V$ and $\hat{\zeta} = \bar{B}^{\pi^E}\zeta$. Then:

$$\begin{aligned}R_0 - \widehat{R} &= -(\bar{B}^{\pi^E}\zeta - \bar{B}^{\hat{\pi}^E}\bar{B}^{\pi^E}\zeta) + (E - \gamma_0P)V - (E - \widehat{\gamma}P)(E - \widehat{\gamma}P)^{-1}(E - \gamma_0P)V \\ &= -(I_{S \times A} - \bar{B}^{\hat{\pi}^E})\bar{B}^{\pi^E}\zeta \\ &= -B^{\hat{\pi}^E}\bar{B}^{\pi^E}\zeta\end{aligned}\tag{32}$$

As the expert-filter-complement $\bar{B}^{\hat{\pi}^E}$ is linear and sums with the expert-filter to unity, i.e., $B^{\hat{\pi}^E} + \bar{B}^{\hat{\pi}^E} = I_{S \times A}$, we get:

$$|R_0 - \widehat{R}| \leq B^{\hat{\pi}^E}\bar{B}^{\pi^E}\zeta.\tag{33}$$

Finally, we obtain $\|\zeta\|_{\infty} \leq \frac{R_{\max}}{1 - \gamma_0}$ by using the condition $\|R_0\| \leq R_{\max}$. \square

B.3 Proof of Theorem 4.7

To prove Theorem 4.7, we need three lemmas.

Lemma B.1 (lemma 1 from Jiang et al. (2015)). *For any MDP M with rewards in $[0, R_{\max}]$, $\forall \pi : S \rightarrow A$ and $\widehat{\gamma} \leq \gamma_0$,*

$$V_{R_0, \widehat{\gamma}}^{\pi} \leq V_{R_0, \gamma_0}^{\pi} \leq V_{R_0, \widehat{\gamma}}^{\pi} + \frac{\gamma_0 - \widehat{\gamma}}{(1 - \gamma_0)(1 - \widehat{\gamma})}R_{\max}\tag{34}$$

Hence, we have the following upper bound:

$$\left\| V_{R_0, \gamma_0}^{\pi_{R_0, \gamma_0}^*} - V_{R_0, \widehat{\gamma}}^{\pi_{R_0, \widehat{\gamma}}^*} \right\|_{\infty} \leq \frac{\gamma_0 - \widehat{\gamma}}{(1 - \gamma_0)(1 - \widehat{\gamma})}R_{\max}\tag{35}$$

Intuitively, Lemma B.1 measures the performance discrepancy of a policy π when evaluated under two different discount factors: $\hat{\gamma}$ and γ_0 .

Lemma B.2 (Adapted from lemma 3 in Jiang et al. (2015)). *For any $M = (S, A, P, \hat{R}, \hat{\gamma})$ with \hat{R} bounded by $[0, R_{max}]$,*

$$\left\| V_{R_0, \hat{\gamma}}^{\pi_{R_0, \hat{\gamma}}} - V_{R_0, \hat{\gamma}}^{\pi_{\hat{R}, \hat{\gamma}}} \right\|_{\infty} \leq 2 \max_{\pi \in \Pi_{\hat{\gamma}}} \left\| V_{R_0, \hat{\gamma}}^{\pi} - V_{\hat{R}, \hat{\gamma}}^{\pi} \right\|_{\infty} \quad (36)$$

Proof. $\forall s \in S$,

$$\begin{aligned} & V_{R_0, \hat{\gamma}}^{\pi_{R_0, \hat{\gamma}}} (s) - V_{R_0, \hat{\gamma}}^{\pi_{\hat{R}, \hat{\gamma}}} (s) \\ &= (V_{R_0, \hat{\gamma}}^{\pi_{R_0, \hat{\gamma}}} (s) - V_{\hat{R}, \hat{\gamma}}^{\pi_{R_0, \hat{\gamma}}} (s)) - (V_{R_0, \hat{\gamma}}^{\pi_{\hat{R}, \hat{\gamma}}} (s) - V_{\hat{R}, \hat{\gamma}}^{\pi_{\hat{R}, \hat{\gamma}}} (s)) + (V_{\hat{R}, \hat{\gamma}}^{\pi_{R_0, \hat{\gamma}}} (s) - V_{\hat{R}, \hat{\gamma}}^{\pi_{\hat{R}, \hat{\gamma}}} (s)) \\ &\leq (V_{R_0, \hat{\gamma}}^{\pi_{R_0, \hat{\gamma}}} (s) - V_{\hat{R}, \hat{\gamma}}^{\pi_{R_0, \hat{\gamma}}} (s)) - (V_{R_0, \hat{\gamma}}^{\pi_{\hat{R}, \hat{\gamma}}} (s) - V_{\hat{R}, \hat{\gamma}}^{\pi_{\hat{R}, \hat{\gamma}}} (s)) \\ &\leq 2 \max_{\pi \in \Pi_{\hat{\gamma}}} |V_{R_0, \hat{\gamma}}^{\pi} (s) - V_{\hat{R}, \hat{\gamma}}^{\pi} (s)|. \end{aligned} \quad (37)$$

□

Intuitively, Lemma B.2 measures the difference between V-functions of two policies: the optimal policy under the ground-truth reward function R_0 , and the one under the estimated reward function \hat{R} . Both are evaluated using R_0 and the effective discount factor $\hat{\gamma}$. Lemma B.2 shows that this difference is at most double the highest V-function difference among policies in $\Pi_{\hat{\gamma}}$, when evaluated with R_0 and \hat{R} . This connects the value difference between two optimal policies evaluated under the ground truth reward to the difference in the same policy evaluated using the ground truth and estimated rewards respectively.

Lemma B.3. *Let $\mathcal{M} = (S, A, P)$ be a partial MDP, and let $R_0 \in \mathbb{R}_{\geq 0}^{S \times A}$ be the ground-truth reward function and $\hat{R} \in \mathbb{R}_{\geq 0}^{S \times A}$ be the estimated reward function with the discount factor $\hat{\gamma}$, and let π be a policy. Then the following inequality holds:*

$$\left\| V_{R_0, \hat{\gamma}}^{\pi} - V_{\hat{R}, \hat{\gamma}}^{\pi} \right\|_{\infty} \leq \frac{1}{1 - \hat{\gamma}} \left\| R_0 - \hat{R} \right\|_{\infty} \quad (38)$$

Proof. From the bellman equation, we have:

$$V_{R_0, \hat{\gamma}}^{\pi} = \pi R_0 + \hat{\gamma} \pi P V_{R_0, \hat{\gamma}}^{\pi}. \quad (39)$$

Rearrange this, we will have $V_{R_0, \hat{\gamma}}^{\pi} = (I_S - \hat{\gamma} \pi P)^{-1} \pi R_0$. Therefore,

$$\begin{aligned} V_{R_0, \hat{\gamma}}^{\pi} - V_{\hat{R}, \hat{\gamma}}^{\pi} &= (I_S - \hat{\gamma} \pi P)^{-1} \pi R_0 - (I_S - \hat{\gamma} \pi P)^{-1} \pi \hat{R} \\ &= (I_S - \hat{\gamma} \pi P)^{-1} \pi (R_0 - \hat{R}) \end{aligned} \quad (40)$$

For the L_{∞} inequality, we simply observe:

$$\begin{aligned} \left\| V_{R_0, \hat{\gamma}}^{\pi} - V_{\hat{R}, \hat{\gamma}}^{\pi} \right\|_{\infty} &= \left\| (I_S - \hat{\gamma} \pi P)^{-1} \pi (R_0 - \hat{R}) \right\|_{\infty} \\ &\leq \left\| (I_S - \hat{\gamma} \pi P)^{-1} \right\|_{\infty} \left\| \pi \right\|_{\infty} \left\| R_0 - \hat{R} \right\|_{\infty} \\ &\leq \frac{1}{1 - \hat{\gamma}} \left\| R_0 - \hat{R} \right\|_{\infty} \end{aligned} \quad (41)$$

where we exploited the fact that $\left\| (I_S - \hat{\gamma} \pi P)^{-1} \right\|_{\infty} = \frac{1}{1 - \hat{\gamma}}$ and that $\left\| \pi \right\|_{\infty} \leq 1$. □

Using these three lemmas, we can now proceed to prove Theorem 4.7.

Proof. **Proof of Theorem 4.7** $\forall s \in S$

$$V_{R_0, \gamma_0}^{\pi_{R_0, \gamma_0}^*}(s) - V_{R_0, \hat{\gamma}}^{\pi_{R_0, \hat{\gamma}}^*}(s) = (V_{R_0, \gamma_0}^{\pi_{R_0, \gamma_0}^*}(s) - V_{R_0, \hat{\gamma}}^{\pi_{R_0, \gamma_0}^*}(s)) + (V_{R_0, \hat{\gamma}}^{\pi_{R_0, \gamma_0}^*}(s) - V_{R_0, \hat{\gamma}}^{\pi_{R_0, \hat{\gamma}}^*}(s)). \quad (42)$$

Using Lemma B.1, we obtain:

$$\left\| V_{R_0, \gamma_0}^{\pi_{R_0, \gamma_0}^*} - V_{R_0, \hat{\gamma}}^{\pi_{R_0, \gamma_0}^*} \right\|_{\infty} \leq \frac{\gamma_0 - \hat{\gamma}}{(1 - \gamma_0)(1 - \hat{\gamma})} R_{max}. \quad (43)$$

For the second term, we derive the following:

$$\begin{aligned} V_{R_0, \hat{\gamma}}^{\pi_{R_0, \gamma_0}^*}(s) - V_{R_0, \hat{\gamma}}^{\pi_{R_0, \hat{\gamma}}^*}(s) &\leq V_{R_0, \hat{\gamma}}^{\pi_{R_0, \gamma_0}^*}(s) - V_{R_0, \hat{\gamma}}^{\pi_{R_0, \hat{\gamma}}^*}(s) \\ &\leq V_{R_0, \hat{\gamma}}^{\pi_{R_0, \hat{\gamma}}^*}(s) - V_{R_0, \hat{\gamma}}^{\pi_{R_0, \hat{\gamma}}^*}(s) \\ &\leq 2 \max_{\pi \in \Pi_{\hat{\gamma}}} |V_{R_0, \hat{\gamma}}^{\pi}(s) - V_{R_0, \hat{\gamma}}^{\pi_{R_0, \hat{\gamma}}^*}(s)|. \end{aligned} \quad (44)$$

The first line results from $\hat{\gamma} \leq \gamma_0$, the second line from $V_{R_0, \hat{\gamma}}^{\pi_{R_0, \hat{\gamma}}^*}(s) \geq V_{R_0, \hat{\gamma}}^{\pi_{R_0, \gamma'}^*}(s)$ for any $\gamma' \in [0, 1]$, and the last line utilizes Lemma B.2.

Using Lemma B.3, for any policy π , we get:

$$\left\| V_{R_0, \hat{\gamma}}^{\pi} - V_{R_0, \hat{\gamma}}^{\pi_{R_0, \hat{\gamma}}^*} \right\|_{\infty} \leq \frac{1}{1 - \hat{\gamma}} \left\| R_0 - \hat{R} \right\|_{\infty} \quad (45)$$

By combining Equations 44 and 45, we arrive at the inequality:

$$\left\| V_{R_0, \hat{\gamma}}^{\pi_{R_0, \gamma_0}^*} - V_{R_0, \hat{\gamma}}^{\pi_{R_0, \hat{\gamma}}^*} \right\|_{\infty} \leq \frac{2}{1 - \hat{\gamma}} \left\| R_0 - \hat{R} \right\|_{\infty} \quad (46)$$

□

B.4 Proof of Theorem 4.1

Proof. **Proof of Theorem 4.1** Recall from Theorem 4.6 that the reward function estimation error, denoted by $\left\| R_0 - \hat{R} \right\|$, is upper-bounded by $\bar{B}^{\pi^E} B^{\hat{\pi}^E} \zeta$. Here, $B^{\hat{\pi}^E}(\cdot)$ represents the *expert-filter* that preserves function values only for actions taken by the approximate expert policy $\hat{\pi}^E(a|s)$, while $\bar{B}^{\pi^E}(\cdot)$ is the *expert-filter-complement* that preserves values for actions not taken by the ground-truth expert policy $\pi^E(a|s)$. We use $\left\| \bar{B}^{\pi^E} B^{\hat{\pi}^E} \zeta \right\|_{\infty}$ to measure the global estimation error of the expert policy: as $\hat{\pi}^E$ approaches π^E , most entries of $\bar{B}^{\pi^E} B^{\hat{\pi}^E} \zeta$ become zero, resulting in $\left\| \bar{B}^{\pi^E} B^{\hat{\pi}^E} \zeta \right\|_{\infty}$ converging to zero.

We bound the global expert policy estimation error $\left\| \bar{B}^{\pi^E} B^{\hat{\pi}^E} \zeta \right\|_{\infty}$ using Hoeffding's inequality. Consider N independent $(s_i, \pi^E(s_i))$ expert pairs, with each pair covering one state. For each sample $(s_i, \pi^E(s_i))$ from expert demonstrations, we let $a_i^j = \pi^E(s_i)$ represent the expert action, and its corresponding policy matrix $\hat{\pi}_i^E$ be a $|S| \times |A|$ matrix with $[\hat{\pi}_i^E]_{i,j} = 1$ and zeros elsewhere. The estimated expert policy matrix $\hat{\pi}^E$ is obtained from N such sampled matrices. As N increases, our estimated expert policy converges to the ground-truth expert policy, i.e., $\hat{\pi}^E \rightarrow \pi^E$. Note that $\bar{B}^{\pi^E} B^{\hat{\pi}^E} \zeta(s, a)$ is bounded in $[0, \frac{R_{max}}{1 - \hat{\gamma}}]$. Applying Hoeffding's inequality, given expert samples covering N states, we obtain

$$\Pr \left(\left\| \bar{B}^{\pi^E} B^{\hat{\pi}^E} \zeta \right\|_{\infty} - 0 > t \right) \leq 2 \exp \left\{ - \frac{2Nt^2}{(R_{max}/(1 - \hat{\gamma}))^2} \right\}. \quad (47)$$

In equation (47), the error bound decreases with increasing N and becomes 0 when $N = |S|$. This occurs because as N approaches the size of the state space ($N \rightarrow |S|$), the estimated expert policy

converges to the ground-truth expert policy ($\hat{\pi}^E \rightarrow \pi^E$), rendering most entries of the expert filter term zero. When $\hat{\pi}^E = \pi^E$, all entries of the expert filter term become zero, making $\left\| \bar{B}^{\pi^E} B^{\hat{\pi}^E} \zeta \right\|_{\infty}$ exactly 0. $\left\| \bar{B}^{\pi^E} B^{\hat{\pi}^E} \zeta \right\|_{\infty}$ approaching 0 as $N \rightarrow |S|$ is independent of Hoeffding's inequality. In particular, it does not depend on the asymptotics of Hoeffding's bound, which only tries to capture the sampling variance.

Next, we set the RHS of equation 47 to $\frac{\delta}{|S||\Pi_{\hat{\gamma}}|}$ and we solve for t :

$$\begin{aligned}
2 \exp\left\{-\frac{2Nt^2}{(R_{\max}/(1-\hat{\gamma}))^2}\right\} &= \frac{\delta}{|S||\Pi_{\hat{\gamma}}|} \\
\frac{2Nt^2}{(R_{\max}/(1-\hat{\gamma}))^2} &= \log \frac{|S||\Pi_{\hat{\gamma}}|}{2\delta} \\
t &= \sqrt{\frac{(R_{\max}/(1-\hat{\gamma}))^2}{2N} \log \frac{|S||\Pi_{\hat{\gamma}}|}{2\delta}} \\
t &= \frac{R_{\max}}{1-\hat{\gamma}} \sqrt{\frac{1}{2N} \log \frac{|S||\Pi_{\hat{\gamma}}|}{2\delta}} \tag{48}
\end{aligned}$$

Substitute t into equation 5:

$$\begin{aligned}
&\left\| V_{R_0, \gamma_0}^{\pi_{R_0, \gamma_0}^*} - V_{R_0, \gamma_0}^{\pi_{\hat{R}, \hat{\gamma}}^*} \right\|_{\infty} \\
&\leq \frac{\gamma_0 - \hat{\gamma}}{(1-\gamma_0)(1-\hat{\gamma})} R_{\max} + \frac{2}{1-\hat{\gamma}} \left\| R_0 - \hat{R} \right\|_{\infty} \\
&\leq \frac{\gamma_0 - \hat{\gamma}}{(1-\gamma_0)(1-\hat{\gamma})} R_{\max} + \frac{2}{1-\hat{\gamma}} \left\| \bar{B}^{\pi^E} B^{\hat{\pi}^E} \zeta \right\|_{\infty} \\
&\leq \frac{\gamma_0 - \hat{\gamma}}{(1-\gamma_0)(1-\hat{\gamma})} R_{\max} + \frac{2}{1-\hat{\gamma}} \frac{R_{\max}}{1-\hat{\gamma}} \sqrt{\frac{1}{2N} \log \frac{|S||\Pi_{\hat{\gamma}}|}{2\delta}} \\
&= \frac{\gamma_0 - \hat{\gamma}}{(1-\gamma_0)(1-\hat{\gamma})} R_{\max} + \frac{2R_{\max}}{(1-\hat{\gamma})^2} \sqrt{\frac{1}{2N} \log \frac{|S||\Pi_{\hat{\gamma}}|}{2\delta}}, \tag{49}
\end{aligned}$$

with probability $1 - \delta$.

□

C Details of the Tasks

All tasks share a common action space, transition function with 9 actions per state, and a 10% chance of moving randomly.

Gridworld-simple. In each Gridworld-simple environment, there are 10×10 states with 4 randomly selected goal states. The ground-truth reward function assigns +1 for goal states and 0 for all others. The expert policy moves greedily towards the nearest goal.

Gridworld-hard. The Gridworld-hard environment consists of 15×15 states and 6 random goal states. It has a larger state space and more goal states than Gridworld-simple, but shares the same reward function.

Objectworld-linear. Each Objectworld-linear environment has 10×10 states and 10 randomly placed objects, each with a randomly assigned inner and outer color from the set $C = \{c_0, c_1\}$. Object states receive a reward of +3 for outer color c_0 and +1 for outer color c_1 . All other states have a 0 reward.

Objectworld-nonlinear. Objectworld-nonlinear differs from its linear counterpart only in the reward function. The reward depends on the outer colors of surrounding objects: +1 for states within 3 grids of c_0 and 2 grids of c_1 , -1 for states within 3 grids of c_1 , and 0 otherwise.

D Modifications to the Linear Programming IRL method (LP-IRL)

The original objective function of LP-IRL (Ng & Russell, 2000) is formulated on the full state coverage of the expert policy and the ground-truth γ_0 . We modified the objective function to extend it to our setting with varying partial state coverage and $\hat{\gamma}$. W.L.O.G, let a_1 be the uniquely optimal action for all states. The transition probability vector at state s for the expert action is thus $P_{a_1}(s) = P(\cdot|s, a_1)$, while that for the rest of the actions $a \in \{a_2, \dots, a_k\}$ be $P_a(s) = P(\cdot|s, a)$. Our modified objective function for LP-IRL is as follows:

Given expert demonstrations covering N states,

$$\begin{aligned} \max_{\hat{R}} \sum_{i=1}^N \min_{a \in \{a_2, \dots, a_k\}} (P_{a_1}(i) - P_a(i))(I - \hat{\gamma}\hat{P}_{a_1})^{-1}\hat{R} \\ \text{subject to } (P_{a_1}(i) - P_a(i))(I - \hat{\gamma}\hat{P}_{a_1})^{-1}\hat{R} \geq b \\ b > 0, \forall a \in \{a_2, \dots, a_k\} \\ |\hat{R}| \leq R_{max}, \text{ for } i = 1, \dots, N, \end{aligned} \quad (50)$$

whereas P_{a_1} is full expert policy transition matrix of size $|S| \times |S|$ such that $[P_{a_1}](s, s') = P(s'|a_1, s)$, while \hat{P}_{a_1} is an estimate of P_{a_1} from partial expert demonstrations covering only $N \leq |S|$ states. Essentially, the transition matrix of the expert policy P_{a_1} is the combination of the transition function P (known) and the expert policy π^E (unknown). Therefore, estimating transition matrix of the expert policy \hat{P}_{a_1} is equivalent to estimating the expert policy from expert demonstrations. Our modifications are highlighted below.

Estimate Expert Transition Matrix. We estimate \hat{P}_{a_1} by setting the transitions of the undemonstrated states to 0. Using this estimation, the action choices at the undemonstrated states do not affect the constraints on the other states. In addition, the value of the undemonstrated state myopically reduced to the state reward function.

Use Different Discount Factors. Our objective function also allows $\hat{\gamma}$ to differ from the ground-truth γ_0 . That is, with an estimated \hat{P}_{a_1} , we allow the mapping $\hat{F}_{i, \hat{\gamma}} = (P_{a_1}(i) - P_a(i))(I - \hat{\gamma}\hat{P}_{a_1})^{-1}$ to take different $\hat{\gamma}$ s to account the temporal effect of the policy at different horizons.

Remove L1 Regularization. The original LP-IRL uses the L_1 -regularization on the reward function, i.e., $|R|$, to resolve the ambiguity among the feasible reward functions. This assumption on the preferred reward function form can be a confounding factor to the performance of the induced policy, therefore we remove it to focus on the effect of horizons.

Enforce Uniquely Optimal Expert Policy. To enforce the induced policy to be uniquely optimal, we modified the constraints to be strictly positive, i.e., $b > 0$.

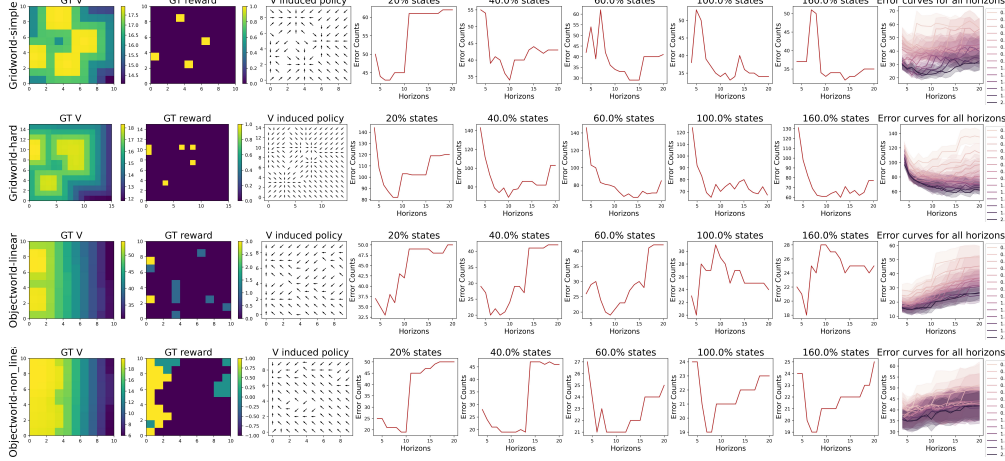
E Modifications to the Maximum Entropy IRL method (MaxEnt-IRL)

Our theoretical analysis of the effective horizon stems from the error bound between two feasible reward function sets: the ground truth expert policy set and the approximated expert policy set derived from limited expert demonstrations. However, most IRL algorithms, such as Maximum Entropy IRL (Ziebart et al., 2008) and Maximum Margin IRL (Ratliff et al., 2006), obtain a single reward function from the feasible set using specific criteria. The error bound between the learned reward function and the ground-truth R_0 may deviate from the bound between their corresponding feasible sets. In this section, we extend our theoretical insights to Maximum Entropy Inverse Reinforcement Learning (Ziebart et al., 2008) and demonstrate that our conclusions on the effective horizon are still applicable when choosing the reward function based on specific criteria.

E.1 Maximum Entropy IRL

MaxEnt-IRL is formulated for finite horizon MDPs with horizon T_0 and no discounting. The reward function is linear in the state feature, i.e., $r = \theta^{T_0} \phi(s)$. The reward of a trajectory $\tau = (s_0, \dots, s_{T_0})$ is the undiscounted sum of all state rewards, where f_{T_0} is the total feature count for the trajectory τ . MaxEnt IRL aims to match the feature counts between the policy and the expert demonstrations while

Table 2: Summary of MaxEnt-IRL with different horizons for the four tasks. For each task, we present the ground-truth value function (column 1), ground-truth reward function (column 2), expert policy (column 3), error count curves in all states for different expert data coverage levels for a **single instance** of the task (columns 4-8), and finally, a summary of the error curves for a **batch** of 10 MDPs (column 9). In all four tasks, the ground-truth horizon $T_0 = 20$. The optimal horizon $\hat{T}^* < T_0$ for varying expert data coverage.



maximizing the entropy of the induced policy. This leads to a distribution over behaviors constrained to match feature expectations, as shown in Equation (51).

$$p(\tau|\theta, P, T_0) \approx \frac{1}{Z(\theta, P, T_0)} \exp^{\theta^T f_{T_0}} \prod_{s_t, a_t, s_{t+1} \in \tau} P(s_{t+1}|s_t, a_t) \quad (51)$$

The MaxEnt IRL objective is to choose the reward parameter θ that maximizes the probability of expert demonstrations under the distribution in Equation (51):

$$\theta^* := \arg \max_{\theta} L(\theta) = \arg \max_{\theta} \sum_{\tau_i \in demo} \log p(\tau_i|\theta, P, T_0) \quad (52)$$

The objective function in equation (52) can be optimized using gradient-based methods, where the gradient is the difference between the empirical and learner’s expected feature counts, expressed in terms of expected state visitation frequencies, D_{s_i, T_0} .

$$\nabla L(\theta) = \tilde{f} - \sum_{\tau \in demo} p(\tau|\theta, P) f_{T_0} = \tilde{f} - \sum_{s_i} D_{s_i, T_0} f_{s_i} \quad (53)$$

E.2 Maximum Entropy IRL with varying Effective Horizon

To extend MaxEnt IRL to varying effective horizons, we optimize trajectories with horizon $\hat{T} \leq T_0$. The corresponding optimal trajectory distribution is given in Equation (54), where $f_{\hat{T}}$ is the undiscounted sum of \hat{T} consecutive states in trajectory $\tau = (s_0, \dots, s_{\hat{T}})$.

$$p(\tau|\theta, P, \hat{T}) \approx \frac{1}{Z(\theta, P, \hat{T})} \exp^{\theta^T f_{\hat{T}}} \prod_{t=0}^{\hat{T}-1} P(s_{t+1}|s_t, a_t) \quad (54)$$

whereas the feature factor $f_{\hat{T}} = \sum_{t=0}^{\hat{T}-1} \phi(s_t)$ is the undiscounted sum of \hat{T} consecutive states in trajectory $\tau = (s_0, \dots, s_{\hat{T}})$.

To investigate the performance of varying effective horizons under the same data coverage, we adjust the expert trajectories’ lengths to match the planning horizons \hat{T} , while maintaining the total number

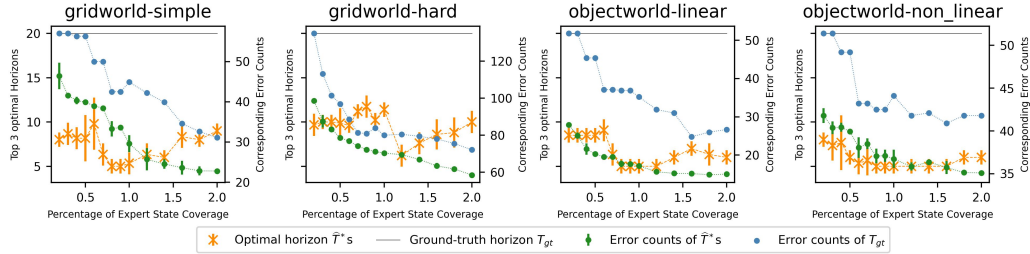


Figure 3: Optimal horizons (\hat{T}^*) for MaxEnt-IRL at varying expert demonstration coverage. We obtain the top 3 \hat{T}^* s for each coverage using the algorithm in Section 5.2. Orange curves show how \hat{T}^* changes with expert coverage, while green curves display corresponding error counts. The ground-truth $T_0 = 20$ is depicted by a grey line, with corresponding error lines in blue. The trends are consistent with LP-IRL.

of demonstrated states constant. Given that the expert covers N states, for each effective horizon \hat{T} , we collect N/\hat{T} trajectories with random initial states. Consequently, the gradient of the objective function is modified as shown in Equation (55):

$$\nabla L(\theta, \hat{T}) = \tilde{f}_{\hat{T}} - \sum_{\tau \in \text{demo}} p(\tau|\theta, P, \hat{T}) f_{\hat{T}} = \tilde{f}_{\hat{T}} - \sum_{s_i} D_{s_i, \hat{T}} f_{s_i} \quad (55)$$

where the expert expected feature vector $\tilde{f}_{\hat{T}}$ and the induced state visitation frequency $D_{s_i, \hat{T}}$ consider only trajectories with length \hat{T} .

Our method for collecting expert demonstrations differs from the standard IRL approaches, where expert demonstrations are fixed and given upfront. Instead, we generate expert trajectories independently for each horizon \hat{T} by rolling out trajectories with random initial states using the expert policy.

An alternative approach is to augment the fixed set of expert trajectories with length T_0 by breaking them into $T_0 - \hat{T} + 1$ shorter segments each with length \hat{T} . However, this method can slightly underestimate the visitation frequency of the final states of the original trajectories due to uniform sampling over the first $T_0 - \hat{T} + 1$ states. Our data collection method eliminates the potential bias that may arise from the quality of the expert demonstrations. In addition, our initial state distribution ρ_0 is a uniform distribution over the entire state space, which ensures a good approximation of the true state visitation frequency of the expert policy.

E.3 Results

The performance trends of MaxEnt-IRL align with those of LP-IRL, further supporting our theoretical results. Table 2 provides a summary of the performance. Figure 3 demonstrates how the optimal horizon \hat{T}^* changes with increasing expert coverage for MaxEnt-IRL. Figure 4 summarizes cross-validation results for MaxEnt-IRL.

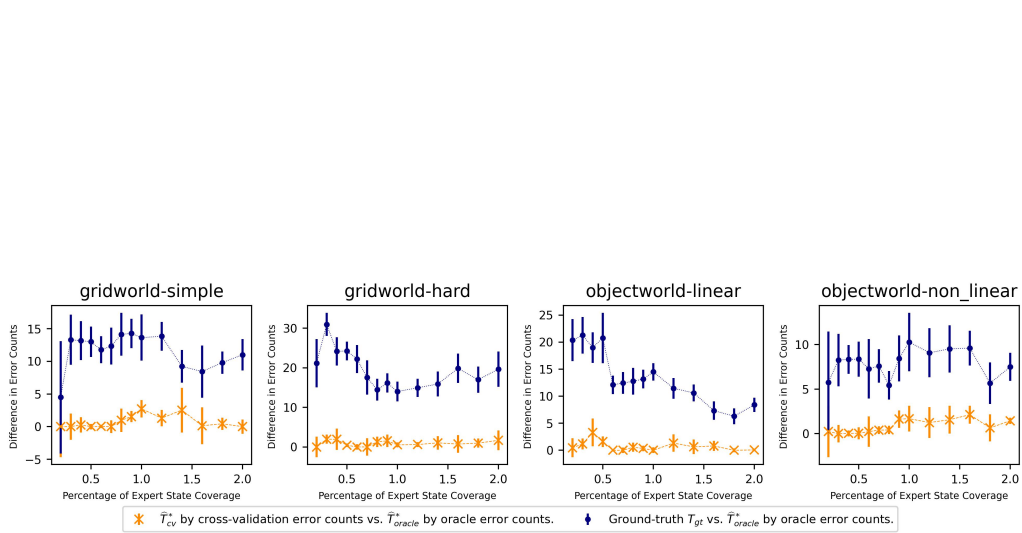


Figure 4: Cross-validation results for four tasks on MaxEnt-IRL. The x -axis represents expert demonstration coverage, while the y -axis shows error count differences in all states for various \hat{T}^* : \hat{T}_{cv}^* learned via cross-validation, and \hat{T}_{oracle}^* chosen optimally using the oracle. Orange dots depict error count differences between the induced policies of \hat{T}_{cv}^* and \hat{T}_{oracle}^* , while blue dots represent differences between the induced policies of T_0 and \hat{T}_{oracle}^* .